Astronomy Letters, Vol. 30, No. 11, 2004, pp. 759–771. Translated from Pis'ma v Astronomicheskiĭ Zhurnal, Vol. 30, No. 11, 2004, pp. 835–847.

Symmetry of the Neutron and Proton Superfluidity Effects in Cooling Neutron Stars

M. E. Gusakov[1], A. D. Kaminker[1*], D. G. Yakovlev[1], and O. Yu. Gnedin[2]

[1] *Ioffe Physicotechnical Institute, Russian Academy of Sciences, ul. Politekhnicheskaya 26, St. Petersburg, 194021 Russia*

[2] *Space Telescope Science Institute, 3700 San Martin Drive, Baltimore, MD 21218, USA*

Received April 2, 2004

Abstract—We investigate the combined effect of neutron and proton superfluidities on the cooling of neutron stars whose cores consist of nucleons and electrons. We consider the singlet state paring of protons and the triplet pairing of neutrons in the cores of neutron stars. The critical superfluid temperatures T_c are assumed to depend on the matter density. We study two types of neutron pairing with different components of the total angular momentum of a Cooper pair along the quantization axis ($|m_J| = 0$ or 2). Our calculations are compared with the observations of thermal emission from isolated neutron stars. We show that the observations can be interpreted by using two classes of superfluidity models: (1) strong proton superfluidity with a maximum critical temperature in the stellar core $T_c^{\max} \gtrsim 4 \times 10^9$ K and weak neutron superfluidity of any type ($T_c^{\max} \lesssim 2 \times 10^8$ K); (2) strong neutron superfluidity (pairing with $m_J = 0$) and weak proton superfluidity. The two types of models reflect an approximate symmetry with respect to an interchange of the critical neutron and proton pairing temperatures. © *2004 MAIK "Nauka/Interperiodica".*

Key words: *neutron stars, nucleon superfluidity, thermal emission.*

INTRODUCTION

At present, the properties of superdense matter in the cores of neutron stars are known poorly. For example, the fundamental problem of the equation of state for supernuclear-density matter has not yet been solved. The existing calculations are model dependent and yield a wide variety of equations of state for matter in the cores of neutron stars (Lattimer and Prakash 2001; Haensel 2003) with different compositions of this matter (nucleons, hyperons, pion or kaon condensates, quarks). The properties of nucleon superfluidity in the inner layers of neutron stars are also unclear. The calculated critical nucleon superfluidity temperatures strongly depend on the nucleon–nucleon interaction model used and on the method of allowance for many-body effects (see, e.g., Lombardo and Schulze 2001). In particular, they can be studied by comparing the star cooling theory with the observations of thermal emission from isolated neutron stars.

Here, we continue to simulate the cooling of superfluid neutron stars whose cores contain neutrons, protons, and electrons and whose critical nucleon superfluidity temperatures depend on the matter density. We extend the class of cooling models that were proposed by Kaminker *et al.* (2001, 2002) and Yakovlev *et al.* (2001a, 2002) to interpret the observations of thermal emission from isolated neutron stars. These authors paid particular attention to the case of strong proton superfluidity and weak neutron superfluidity in the stellar core. Since the superfluidity models have a large uncertainty, we consider a broader class of models without assuming from the outset that the proton pairing is stronger than the neutron pairing. In addition, attention is given to the nonstandard neutron triplet pairing model with an anisotropic gap that vanishes along the quantization axis.

OBSERVATIONAL DATA

The observational data on thermal emission from eleven isolated middle-aged ($10^3 \lesssim t \lesssim 10^6$ yr) neutron stars are collected in the table. In what follows, T_s^∞ is the stellar surface temperature recorded by a distant observer, and t is the age of the star. The data differ from those presented previously (see, e.g., Yakovlev *et al.* 2002), because they include the results of new observations.

Two young objects, RX J0822–4300 and 1E 1207.4–5209 (=J1210–5226), are radio-quiet neutron stars in supernova remnants. Two of the

*E-mail: kam@astro.ioffe.ru

Surface temperatures of isolated neutron stars

Source	t, 10^3 yr	T_s^∞, 10^6 K	Model[a]	Confidence, %	References
PSR J0205+6449	0.82	<1.1	bb	–	Slane *et al.* (2002)
Crab	1	<2.0	bb	99.7	Weisskopf *et al.* (2004)
RX J0822–4300	2–5	1.6–1.9	H	90	Zavlin *et al.* (1999)
1E 1207.4–5209	3–20	1.4–1.9	H	90	Zavlin *et al.* (2004)
Vela	11–25	0.65–0.71	H	68	Pavlov *et al.* (2001)
PSR B1706–44	~ 17	$0.82^{+0.01}_{-0.34}$	H	68	McGowan *et al.* (2004)
PSR J0538+2817	30 ± 4	~ 0.87	H	–	Zavlin and Pavlov (2003)
Geminga	~ 340	~ 0.5	bb	90	Zavlin and Pavlov (2003)
RX J1856.4–3754	~ 500	<0.65	–	–	see text
PSR B1055–52	~ 540	~ 0.75	bb	–	Pavlov and Zavlin (2003)
RX J0720.4–3125	~ 1300	~ 0.51	H	–	Motch *et al.* (2003)

[a] The observations were interpreted in terms of either a hydrogen atmosphere model (H) or a blackbody model (bb).

three oldest objects ($t \geqslant 5 \times 10^5$ yr), RX J1856.4–3754 and RX J0720.4–3125, are also radio-quiet neutron stars. The remaining seven sources—PSR J0205+6449, the Crab pulsar (PSR B0531+21), the Vela pulsar (PSR B0833–45), PSR B1706–44, PSR J0538+2817, Geminga (PSR B0633+1746), and PSR B1055–52—are observed as radio pulsars. PSR J0205+6449 and the Crab pulsar are located in the remnants of historical supernovae; their ages are known exactly. The age of RX J0822–4300 was determined from the age of the remnant of the parent supernova Puppis A and lies within the range $t = (2–5) \times 10^3$ yr (see, e.g., Arendt *et al.* 1991), with the most probable value being $t = 3.7 \times 10^3$ yr (Winkler *et al.* 1988). The age of 1E 1207.4–5209 is assumed to be equal to the age of the remnant of the parent supernova G296.5+10. According to Roger *et al.* (1988), this age lies within the range $\sim 3 \times 10^3$ to $\sim 20 \times 10^3$ yr. The age of the Vela pulsar is assumed to lie within the range from the standard characteristic pulsar age of 1.1×10^4 yr to the age of 2.5×10^4 yr obtained by Lyne *et al.* (1996) by analyzing the pulsar spindown with allowance made for the observed glitches. Kramer *et al.* (2003) estimated the age of PSR J0538+2817, $t = (30 \pm 4) \times 10^3$ yr, from the measured proper motion of the neutron star relative to the center of the remnant of the parent supernova S147. The age of RX J1856.4–3754 was estimated by Walter (2001) from kinematic considerations and revised by Walter and Lattimer (2002). Following the latter authors, we take a mean value of $t = 5 \times 10^5$ yr and choose an error range for t that excludes the value of $t = 9 \times 10^5$ yr obtained by Walter (2001). Zane *et al.* (2002) and Kaplan *et al.* (2002) estimated the characteristic age of RX J0720.4–3125 from the X-ray measurements of the spindown rate of the star $\dot{P}$. We take a mean value of 1.3×10^6 yr with an uncertainty factor of 2. The ages of the three radio pulsars PSR B1706–44, Geminga, and PSR B1055–52 are set equal to the characteristic age with the same uncertainty factor of 2.

For the two youngest objects (the Crab pulsar and PSR J0205+6449), only upper limits were placed on T_s^∞ (Weisskopf *et al.* 2004; Slane *et al.* 2002). The surface temperatures of five sources—RX J0822–4300, 1E 1207.4–5209, Vela, PSR B1706–44, and PSR J0538+2817—were determined by using neutron-star hydrogen atmosphere models (for references, see the table). These models yield more realistic neutron-star radii and hydrogen column densities (see, e.g., Pavlov *et al.* 2002) than the blackbody model.

The pulsar PSR B0656+14 that was considered previously (see, e.g., Yakovlev *et al.* 2002) was excluded from the table. A simultaneous analysis of new X-ray and optical observations of the source

(given the distance to it improved using the parallax measurements by Brisken *et al.* (2003)) leads either to an overly small neutron-star radius (in the blackbody model) or to an overly small distance to the star (in the hydrogen atmosphere model) (Zavlin and Pavlov 2003). This makes the interpretation of the stellar thermal emission too unreliable.

For Geminga and PSR B1055−52, the blackbody model is more self-consistent. Therefore, we take the values of T_s^∞ obtained by interpreting the observed spectra in terms of this model. For PSR B1055−52, we take T_s^∞ from Pavlov and Zavlin (2003).

The surface temperature of RX J1856.4−3754 has not been determined accurately enough. The wide spread in T_s^∞ obtained for different radiation models (see, e.g., Pons *et al.* 2002; Braje and Romani 2002; Burwitz *et al.* 2003; Pavlov and Zavlin 2003; Trümper *et al.* 2003) stems from the fact that the optical and X-ray observations cannot be described by a single blackbody model. This may be attributable, for example, to the presence of hot spots on the stellar surface. Therefore, we fix only the upper limit of $T_s^\infty < 6.5 \times 10^5$ K that agrees with the value of T_s^∞ obtained both in the model of a Si-ash atmosphere (Pons *et al.* 2002) and in the model of condensed matter on the stellar surface (Burwitz *et al.* 2003). This limit is also consistent with the model of a nonuniform stellar surface temperature distribution proposed by Pavlov and Zavlin (2003). For the latter model, the mean stellar surface temperature is $T_s^\infty = 5 \times 10^5$ K and lies below the chosen upper limit.

Finally, we took the surface temperature of RX J0720.4−3125 from the paper by Motch *et al.* (2003). These authors interpreted the observed spectrum by using a finite-depth hydrogen atmosphere model.

For PSR J0538−2817, PSR B1055−52, and RX J0720.4−3125, the errors in T_s^∞ were not given by the authors (see the table). In all these case, we assume them to be equal to 20%.

NUCLEON SUPERFLUIDITY MODELS AND NEUTRINO EMISSION DUE TO COOPER PROTON PAIRING

The neutron or proton superfluidity can be described by the density profile of the critical temperature, $T_c(\rho)$. Microscopic theories predict (see, e.g., Lombardo and Schulze 2001; for references, see also the review by Yakovlev *et al.* 1999a) the existence of singlet ($^1S_0$) neutron pairing ($T_{cn} = T_{cns}$) in the inner crust and the outermost layers of the stellar core and singlet proton pairing (T_{cp}) and triplet ($^3P_2$) neutron pairing ($T_{cn} = T_{cnt}$) in the stellar core. The possibility of different angular momentum components m_J for a neutron–neutron pair along the quantization axis ($|m_J| = 0, 1, 2$) should be taken into account when triplet pairing is considered. A superposition of states with different m_J can also be an energetically favored state of the Cooper pair (see, e.g., Amundsen and Østgaard 1985; Baldo *et al.* 1992; Khodel *et al.* 1998, 2001). Only one type of triplet superfluidity with $m_J = 0$ has commonly been assumed in neutron-star cooling calculations. The papers by Schaab *et al.* (1998) and Gusakov and Gnedin (2002) constitute an exception. Below, we consider the neutron triplet pairing with $|m_J| = 0$ and 2, because the effects of these two types of superfluidity on the heat capacity and the neutrino luminosity of neutron stars are qualitatively different. Following Yakovlev *et al.* (1999a), we denote the three types of superfluidity ($^1S_0$, $^3P_2(m_J = 0)$, and $^3P_2(|m_J| = 2)$) considered here by the letters A, B, and C, respectively. The energy gap in the neutron energy spectrum, $\varepsilon(\mathbf{p})$, is isotropic in case A and anisotropic in cases B and C; i.e., it depends on the angle between the direction of the particle momentum $\mathbf{p}$ and the quantization (z) axis. In case C, the energy gap vanishes if $\mathbf{p}$ is directed along the z axis.

Nucleon superfluidity suppresses the neutrino processes involving nucleons, changes the nucleon heat capacity, and triggers an additional neutrino emission mechanism related to the Cooper nucleon pairing (Flowers *et al.* 1976). In this case, the effect of type-C neutron superfluidity on the heat capacity of the matter and the neutrino reactions differs qualitatively from the effect of type-A or -B superfluidity. Thus, for example, the suppression of the neutrino processes and the heat capacity by type-C superfluidity and type-B or -A superfluidity has power-law and exponential dependences, respectively (see, e.g., Yakovlev *et al.* 1999a).

Microscopic theories yield a wide variety of $T_c(\rho)$ profiles (see, e.g., Lombardo and Schulze 2001). The $T_c(\rho)$ maxima can take on values from $\lesssim 10^8$ to 5×10^{10} K. The $T_{cnt}(\rho)$ maxima in many models are lower than the $T_{cp}(\rho)$ and $T_{cns}(\rho)$ maxima, because the attraction between triplet-state nucleons is weaker.

We use four phenomenological model superfluidity profiles $T_c(\rho)$ (for both neutrons and protons) in the core of a neutron star. In Fig. 1, these models are denoted by *a*, *b*, *c*, and *d*. The chosen $T_c(\rho)$ profiles are similar and differ only in height (maximum value): $T_c^{max} = 10^{10}$, 4.0×10^9, 8.0×10^8, and 8.0×10^7 K (models *a*, *b*, *c*, and *d*). Superfluidities *a*, *b*, *c*, and *d* will be called *strong*, *moderately strong*, *moderate*, and *weak*, respectively. The chosen models are consistent with the theoretical calculations of $T_c(\rho)$. The $T_c(\rho)$ curves have steep slopes at $\rho > \rho_D$, where ρ_D is

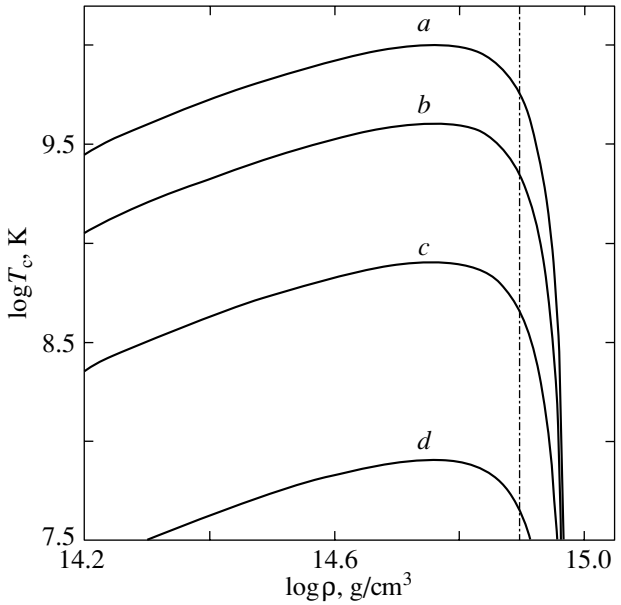

Fig. 1. Model density (ρ) profiles of the critical neutron and/or proton temperatures in the core of a neutron star. The vertical dot-dashed line indicates the threshold density of the direct URCA process.

the threshold density at which the direct URCA process opens (see below).

Below, we denote the combined nucleon superfluidity by $\alpha\beta$, where α is one of the neutron triplet (type B or C) superfluidity models (a, b, c, or d), and β is one of the proton singlet superfluidity models (a, b, c, or d).

Note that there is a large uncertainty in the rate of neutrino energy release Q_p due to Cooper proton pairing. In the nonrelativistic approximation (Yakovlev *et al.* 1999b), $Q_p \propto \zeta_p$, where $\zeta_p = c_{\rm Vp}^2$, and $c_{\rm Vp} \approx 0.08$ is the vector constant of the neutral proton current; the latter is numerically small and leads to very low values of Q_p. For comparison, the rate of neutrino energy release Q_n due to Cooper neutron triplet pairing is proportional to $\zeta_n = c_{\rm Vn}^2 + 2c_{\rm An}^2 = 4.17$, where $c_{\rm Vn} = 1$ and $c_{\rm An} = -1.26$ are the vector and axial vector constants of the neutral neutron current, respectively. According to Kaminker *et al.* (1999), applying the relativistic correction that contains the axial vector constant of the neutral proton current $c_{\rm Ap} = 1.26$ can greatly (by a factor of 10 to 50) increase the rate constant ζ_p (and the rate of energy release Q_p) compared to the nonrelativistic value of $\zeta_p = c_{\rm Vp}^2 = 0.0064$.

We used this value of ζ_p enhanced by relativistic effects in our previous neutron-star cooling calculations. At the same time, studying the cooling of stars with density-dependent critical proton temperatures $T_{\rm cp}(\rho)$ (see, e.g., Kaminker *et al.* 2002), we considered only the models of strong proton superfluidity (similar to model a). Such superfluidity arises at early cooling stages. The neutrino emission due to Cooper proton pairing at these stages cannot compete with other neutrino processes and plays no special role. In a cooler star, this neutrino emission is generated only in small volume and weakly affects the cooling of the star. Thus, in the cooling scenarios with strong proton superfluidity considered previously, the emission due to Cooper proton pairing (and the exact value of ζ_p) was unimportant.

In this paper, we also consider the models of moderate proton superfluidity in which the emission due to Cooper proton pairing can appreciably affect the star cooling and the value of the rate constant ζ_p is important. As was noted, for example, by Yakovlev *et al.* (1999b) and Kaminker *et al.* (1999), the rate constant ζ_p can be determined not only by relativistic effects, but also by the renormalization effects of the medium (many-body effects in nucleon matter). This renormalization for the process in question has not been made. Carter and Prakash (2002) gave an example of a similar renormalization of the constant of the axial vector current. For the sake of definiteness, we perform calculations by choosing the renormalized value of $\zeta_p = 1$. The sensitivity of our calculations to ζ_p is described below (see also Fig. 7).

THE COOLING OF STARS WITH STRONG PROTON SUPERFLUIDITY

Let us compare the observational data with our calculations of the cooling curves ($T_{\rm s}^{\infty}(t)$ profiles) for neutron stars. The calculations were performed using a code described by Gnedin *et al.* (2001). As in previous papers (mentioned in the Introduction), we consider the models of neutron stars whose cores are composed of neutrons n, protons p, and electrons e. We use a moderately stiff equation of state for matter in the stellar core proposed by Prakash *et al.* (1988) (model I with the compression modulus of symmetric nucleon matter at saturation $K = 240$ MeV). The maximum mass of a stable neutron star for the chosen equation of state is $M = 1.977 M_\odot$ (at a radius of $R = 10.754$ km and a central density of $\rho_{\rm c} = 2.575 \times 10^{15}$ g cm^{-3}). This equation of state permits an intense direct URCA process of neutrino generation (Lattimer *et al.* 1991) at densities ρ above the threshold density $\rho_{\rm D} = 7.851 \times 10^{14}$ g cm^{-3}, i.e., in stars with masses $M > M_{\rm D} = 1.358 M_\odot$. The radius of a star with the threshold mass $M_{\rm D}$ is $R = 12.98$ km.

The thermal evolution of a neutron star consists of three stages:

(1) The stage of *thermal relaxation* of the inner stellar layers ($t \lesssim 100$ yr);

(2) The subsequent stage of *neutrino cooling* ($10^2 \lesssim t \lesssim 10^5$ yr) of a star with an isothermal core via neutrino emission from inside the star;

(3) The final stage of *photon cooling* ($t \gtrsim 10^5$ yr) via photon emission from the stellar surface.

The cooling theory for nonsuperfluid stars cannot explain the entire set of observational data (see, e.g., Kaminker *et al.* 2002). However, this theory can be reconciled with the observations by taking into account the possible nucleon superfluidity. According to Kaminker *et al.* (2001), it will suffice to assume the existence of strong proton superfluidity and weak neutron superfluidity in the stellar cores.

Figure 2 shows the cooling curves for neutron stars of different masses with weak neutron superfluidity d and strong proton superfluidity a. Such weak neutron superfluidity switches on only at the photon cooling stage. Therefore, the type of weak neutron superfluidity (B or C) does not affect the cooling of middle-aged stars. The cooling curves for stars with masses $M \gtrsim M_\odot$ fill the hatched region. All of the observed sources fall within this region; i.e., they can be interpreted in terms of the proposed superfluidity model.

As Kaminker *et al.* (2002) showed, strong proton superfluidity with weak neutron superfluidity (or with normal neutrons) gives rise to three types of cooling neutron stars.

Low-mass stars cool down *very slowly* (more slowly than low-mass nonsuperfluid stars). The cooling curves for such stars depend weakly on their mass, the equation of state in their cores, and the proton superfluidity model (on the specific form of the $T_{\rm cp}(\rho)$ profile provided that the superfluidity in the stellar core is strong enough, $T_{\rm cp}(\rho) \gtrsim 4 \times 10^9$ K). The upper boundary of the hatched region in Fig. 2 is the cooling curve for a star with a mass of $M = 1.35 M_\odot$; it is almost indistinguishable from the cooling curve for a star with a mass of $M = 1.1 M_\odot$ and agrees with the observations of four sources, RX J0822−4300, 1E 1207.4−5209, PSR B1055−52, and RX J0720.4−3125, the hottest ones for their ages. These sources will be considered as low-mass neutron stars.

High-mass neutron stars cool down *very rapidly* via intense neutrino emission generated by the direct URCA process in the inner stellar core. At high matter densities ($\rho \gtrsim 10^{15}$ g cm^{-3}), the proton superfluidity weakens (Fig. 1) and ceases to suppress the neutrino emission. The cooling curves for such stars depend weakly on their mass, the equation of state, and the proton superfluidity model. They almost coincide with the cooling curves for high-mass nonsuperfluid stars. All of the observed isolated neutron stars are much hotter than the stars of this type.

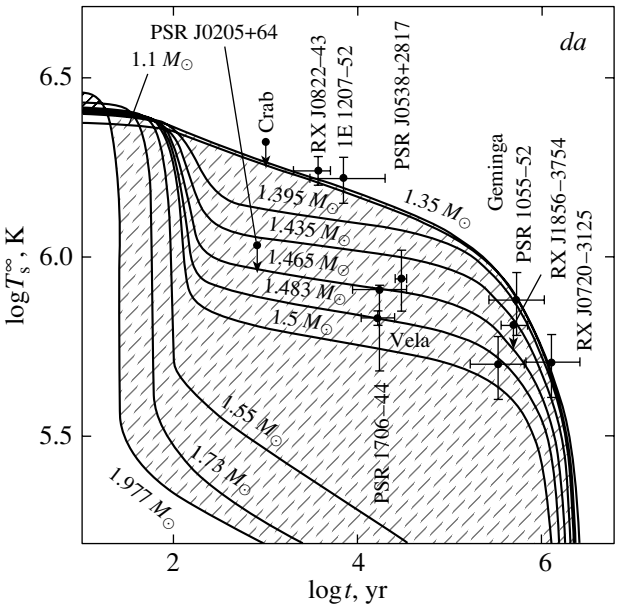

Fig. 2. Comparison of the observations (see the table) with the cooling curves for neutron stars with masses from 1.1 to 1.977 $M_\odot$ (indicated near the curves) for weak neutron superfluidity d and strong proton superfluidity a. The region filled with the cooling curves for stars of different masses is hatched.

Finally, *medium-mass* stars cool down *moderately rapidly*. Their cooling depends strongly on the mass, the equation of state, and the proton superfluidity model. By varying the stellar mass, we can obtain a family of cooling curves that fill the space between the cooling curves for low-mass and high-mass stars. We consider the sources PSR J0205+6449, Vela, PSR B1706−44, PSR J05538+2817, Geminga, and RX J1856.4−3754 as medium-mass stars.

THE COOLING OF NEUTRON STARS WITH COMBINED NUCLEON SUPERFLUIDITY

Figures 3–6 show the cooling curves for neutron stars with different superfluidities of neutrons α and protons β ($\alpha, \beta = a, b, c,$ or d). The neutron superfluidity is of type B. We considered all the possible combinations of neutron and proton superfluidities. The upper cooling curve for a low-mass star ($M = 1.1 M_\odot$, with a central density of $\rho_{\rm c} = 6.23 \times 10^{14}$ g cm^{-3}) and the lower cooling curve for a high-mass star ($M = M_{\rm max}$) are shown for each combination $\alpha\beta$. The lower curve is virtually independent of the models of superfluidity $\alpha\beta$ (see the previous section). The region between the upper and lower cooling curves (similar to the hatched region in Fig. 2) can

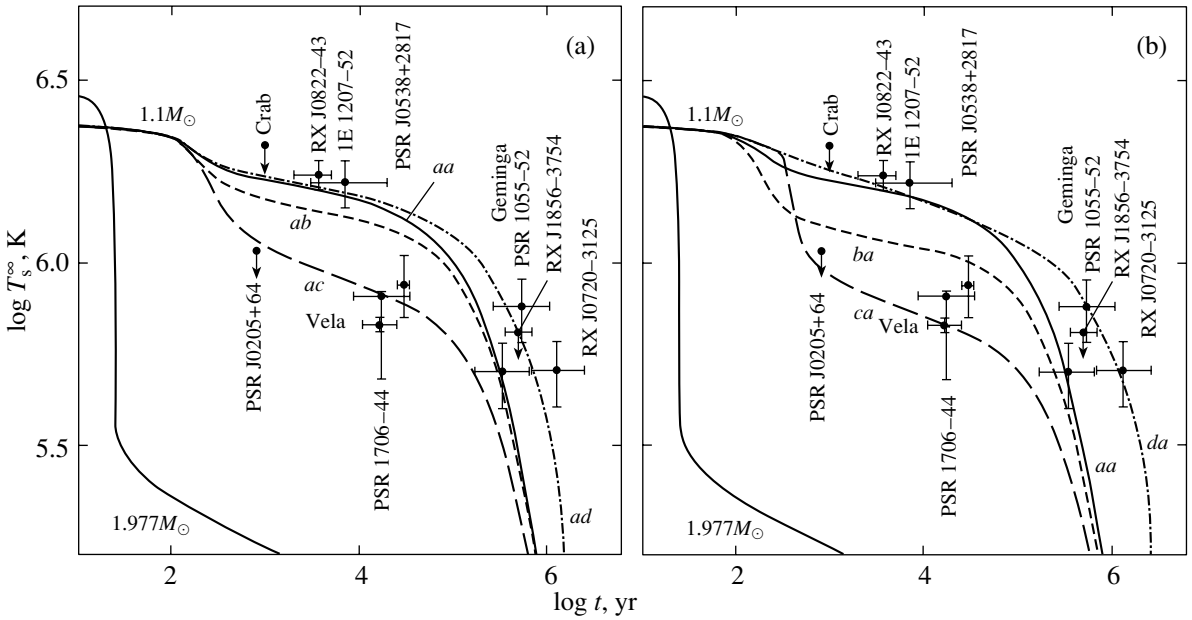

Fig. 3. (a) Cooling curves for stars of two masses, $M = 1.977M_\odot$ and $M = 1.1M_\odot$, with neutron superfluidity a and for different proton superfluidity models (a, b, c, or d); (b) the same for the proton superfluidity model a and different neutron superfluidity models (a, b, c, or d). Type-B neutron superfluidity was chosen for all cases. The theoretical curves are compared with the observations. The cooling of a star with $M = 1.977M_\odot$ does not depend on the superfluidity model.

be filled with the cooling curves of intermediate-mass stars and is admissible for the model of superfluidity $\alpha\beta$ under consideration. As in Fig. 2, the observational data are shown. The nucleon superfluidity models can be constrained by comparing the admissible T_s^∞ regions with the observational data.

Each of Figs. 3–6 consists of two panels: in panel (a), the neutron superfluidity α is fixed, and the cooling curves are given for all four proton superfluidity models; in panel (b), the proton superfluidity β is fixed, and the cooling curves are given for all four neutron superfluidity models. By comparing panels (a) and (b), we can trace the change in cooling when the proton superfluidity is replaced with the neutron superfluidity (and vice versa).

Fixed Proton Superfluidity

Let us choose a proton superfluidity model ($\beta = a, b, c,$ or d) and consider the dependence of the upper cooling curves on the models of neutron superfluidity α in Figs. 3–6.

The $b\beta$ cooling curves run below the $a\beta$ curves because of the neutrino emission due to Cooper neutron pairing. This emission is significantly suppressed in the models with strong neutron superfluidity a (see, e.g., Yakovlev *et al.* 1999a, 1999b, 2001b). All of the remaining neutrino reactions involving neutrons and the neutron heat capacity are completely suppressed by neutron superfluidity a or b. The difference between the $a\beta$ and $b\beta$ cooling curves depends on the model of proton superfluidity β. Thus, for example, as we go from model $\beta = a$ to $\beta = b$ and then to the model of moderate proton superfluidity $\beta = c$, the contribution of the neutrino energy release due to Cooper proton pairing to the neutrino luminosity of the star increases (and becomes dominant for $\beta = c$). Indeed, the neutrino emission due to Cooper pairing affects most strongly the cooling at moderate critical nucleon temperatures, $T_c \sim 2 \times (10^8$–$10^9)$ K (see, e.g., Yakovlev *et al.* 1999b, 2001b). As a result, the difference between the $a\beta$ and $b\beta$ cooling curves in Figs. 3–5 steadily decreases as we go from the model $\beta = a$ to $\beta = b$ and $\beta = c$. At the same time, the admissible theoretical cooling regions agree with the observations increasingly poorly.

For weak superfluidity $\beta = d$ (Fig. 6), the protons remain normal for $t \lesssim 10^5$ yr, until the onset of the photon cooling stage. In this case, the main neutrino process with proton involvement is bremsstrahlung during proton–proton collisions. Since the contribution of this process to the neutrino emission is much smaller than the contribution of the Cooper proton pairing in model c, the difference between the ad and bd curves again increases. As in Fig. 3 (the aa and ba curves), it is determined mainly by the more intense neutrino generation due to Cooper neutron pairing in model b than in model a. As a result, the admissible region of stellar surface temperatures for combined

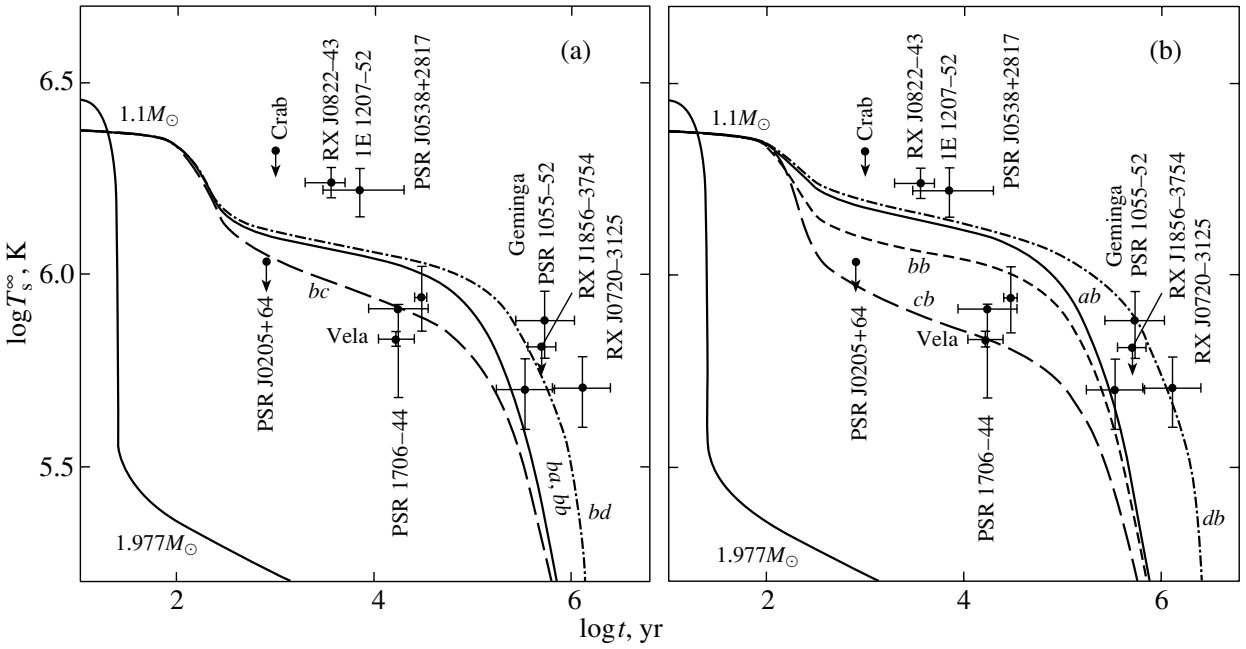

Fig. 4. Same as Fig. 3 for the fixed neutron (a) or proton (b) superfluidity model *b*.

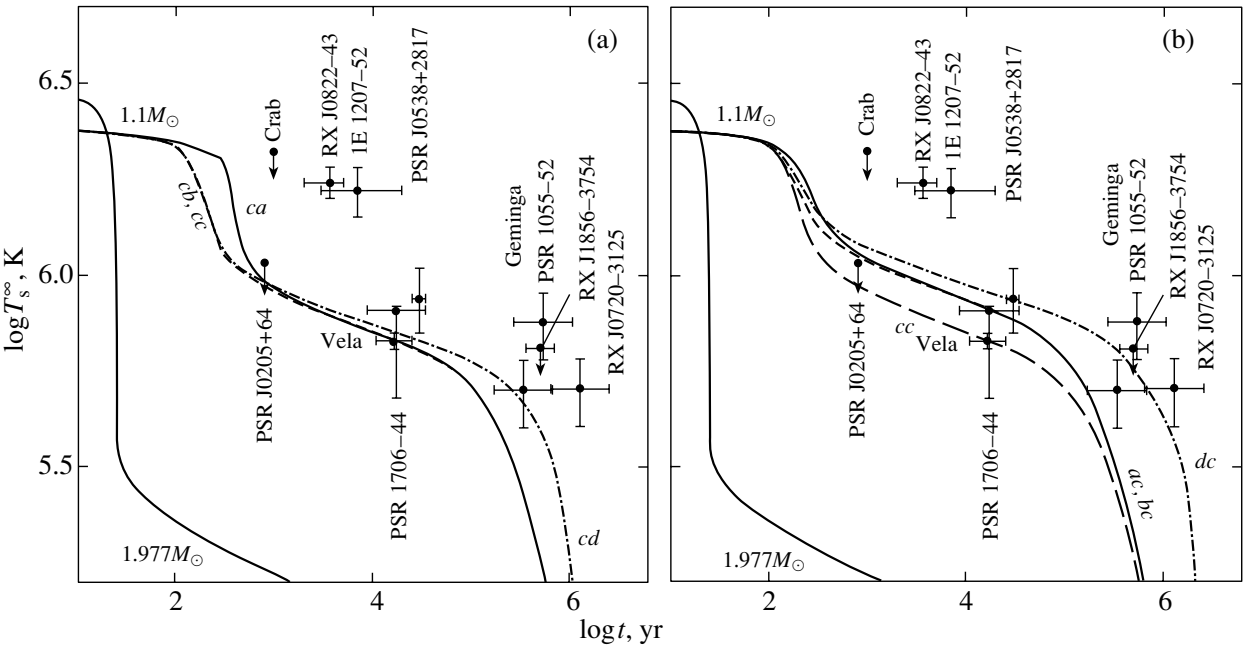

Fig. 5. Same as Fig. 3 for the neutron (a) or proton (b) superfluidity model *c*.

superfluidity *ad* (as in the case of superfluidity *da*, cf. Fig. 6 with Figs. 2 and 3) agrees with the observations.

The $a\beta$ and $b\beta$ curves approach each other at the photon cooling stage ($t \gtrsim 10^5$ yr). In this case, the influence of neutron *a* or *b* superfluidity on the cooling of the star manifests itself mainly in strong suppression of the neutron heat capacity. As a result, the heat capacity of the star is determined by the total heat capacity of the protons (also suppressed by the superfluidity β) and electrons.

For the $c\beta$ superfluidity models, the neutrino emission due to Cooper neutron pairing is particularly effective. As a result, the $c\beta$ cooling curves in Figs. 3–6 run well below the $a\beta$ and $b\beta$ curves and do not differ too much from one another. In particular, all of

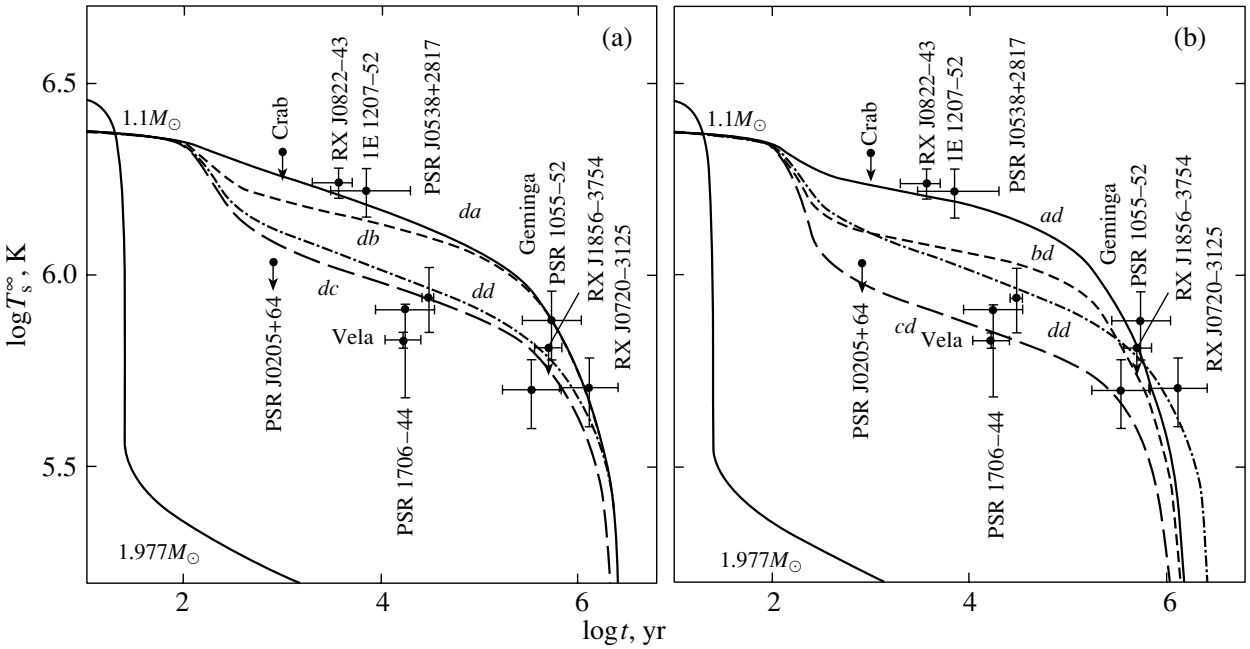

Fig. 6. Same as Fig. 3 for the neutron (a) or proton (b) superfluidity model *d*.

the $c\beta$ curves describe the sharp speedup in cooling at $t \sim 300$ yr attributable to the switch-on of neutrino emission due to neutron pairing. We can see that the admissible stellar surface temperatures obtained for the $c\beta$ superfluidity models lie well below most of the observational data points.

For the model of weak neutron superfluidity *d*, the $d\beta$ curves almost coincide with the cooling curves for normal neutrons. Differences arise only at the photon cooling stage ($t \gtrsim 10^5$ yr) from the partial suppression of the neutron heat capacity. However, at the neutrino cooling stage, the *d*-type neutron superfluidity has not yet set in. Therefore, all of the $d\beta$ cooling curves lie above the $c\beta$ curves. At $t \gtrsim 10^5$–10^6 yr, the $d\beta$ cooling curves for any β run above both the $a\beta$ and $b\beta$ curves due to the strong suppression of the neutron heat capacity by the superfluidities *a* and *b*. Finally, the cooling curve for the model of combined superfluidity *dd* is close to the standard cooling curve for nonsuperfluid low-mass ($M < M_{\rm D}$) neutron stars. This cooling curve disagrees with the observations of many neutron stars (both the hottest and coolest for their ages).

Fixed Neutron Superfluidity

Let us choose a neutron superfluidity model ($\alpha = a, b, c,$ or d) and consider the dependence of the upper cooling curves on the proton superfluidity models β. A comparison of panels (a) and (b) in Figs. 3–6 reveals a qualitative similarity between the cooling curves of low-mass ($M = 1.1M_\odot$) stars when the neutron and proton superfluidities are inverted (i.e., for the models $\alpha\beta$ and $\beta\alpha$).

The quantitative differences between the $\alpha\beta$ and $\beta\alpha$ cooling curves are attributable to different neutron and proton concentrations in the cores of neutron stars and to different types of neutron (triplet) and proton (singlet) pairing. This results in a slightly asymmetric effect of neutrons and protons on the neutrino luminosity and the heat capacity (see, e.g., Yakovlev *et al.* 1999a). Thus, for example, at temperatures T slightly below $T_{\rm c}$, the rate of neutrino energy release due to neutron pairing is approximately an order of magnitude higher than that due to proton pairing (even for the chosen rate constant $\zeta_p = 1$). Therefore, the $b(\beta = a, d)$ and $c(\beta = a, b, d)$ cooling curves (panel (a) in Figs. 4 and 5) lie below the "inverse" $(\alpha = a, d)b$ and $(\alpha = a, b, d)c$ cooling curves (panel (b) in the same figures). On the other hand, the *ad* curve (Fig. 3a) at the photon cooling stage ($t \gtrsim 10^5$ yr) runs below the *da* curve (Fig. 3b). This is because the heat capacity of the neutron-star core is more strongly suppressed by the neutron superfluidity $\alpha = a$ than by the proton superfluidity $\beta = a$. In the remaining cases, the inversion of the neutron and proton superfluidities leads to qualitatively similar (roughly symmetric) cooling curves in Figs. 3–6. For high-mass ($M > M_{\rm D}$) neutron stars, this symmetry was found by Levenfish *et al.* (1999) in their simplified cooling calculations for stars with constant critical neutron and proton temperatures over the stellar core.

A comparison of the upper cooling curves with the observations in Figs. 3–6 shows that there are only

two models of combined nucleon superfluidity that are consistent with the set of observational data. These include the *da* model discussed in the previous section and the "inverse" *ad* model (Figs. 3 and 6). In other words, one (neutron or proton) superfluidity must be weak, while the other must be strong. The remaining models are unable to simultaneously explain the observational data, primarily for four neutron stars (RX J0822−4300, 1E 1207.4−5209, PSR B1055−52, and RX J0720.4−3125), the hottest ones for their ages.

Varying the nucleon superfluidity models, we can constrain the critical nucleon temperatures at which the theory agrees with the observations. In general, the following conditions must be satisfied simultaneously: either $T_{\rm cnt}^{\rm max} \lesssim 2\times10^8$ K and $T_{\rm cp}^{\rm max} \gtrsim 4\times10^9$ K or $T_{\rm cnt}^{\rm max} \gtrsim 5\times10^9$ K and $T_{\rm cp}^{\rm max} \lesssim 2\times10^8$ K.

The models of *moderate neutron and/or proton superfluidity* in the cores of neutron stars with maximum temperatures $T_{\rm cnt}^{\rm max}$ and/or $T_{\rm cp}^{\rm max}$ in the range $\sim (2\times10^8{-}4\times10^9)$ K are inconsistent with the observations of the hottest neutron stars for their ages. We can show that this conclusion is valid for a much broader class of nucleon superfluidity models than those used here (see above). Nevertheless, there is a narrow region of nucleon superfluidity parameters at which the combination of strong nucleon superfluidity of one type and moderate nucleon superfluidity of another type can be reconciled with the observations (see Gusakov *et al.*).

Rate Constant of Neutrino Energy Release due to Cooper Proton Pairing

Let us briefly discuss the sensitivity of the cooling curves to the constant ζ_p in the expression for the rate of neutrino energy release due to Cooper proton pairing. Recall that the value of ζ_p that includes many-body effects is known poorly. In our calculations, we used the (renormalized) value of $\zeta_p = 1$.

As an example, Fig. 7 shows the cooling curves of a low-mass neutron star for three neutron and proton superfluidity models (*db*, *dc*, and *bc*). As was shown above, the neutrino emission due to Cooper pairing is particularly important precisely in low-mass stars. As everywhere in this section, we consider the type-B neutron superfluidity. The lower of the two curves for each superfluidity model was computed with the renormalized constant $\zeta_p = 1$, while the upper curve was computed with the nonrenormalized constant (but obtained by taking into account relativistic effects; see Kaminker *et al.* 1999).

In the *db* model, the proton superfluidity *b* is moderately strong and arises at an early cooling stage.

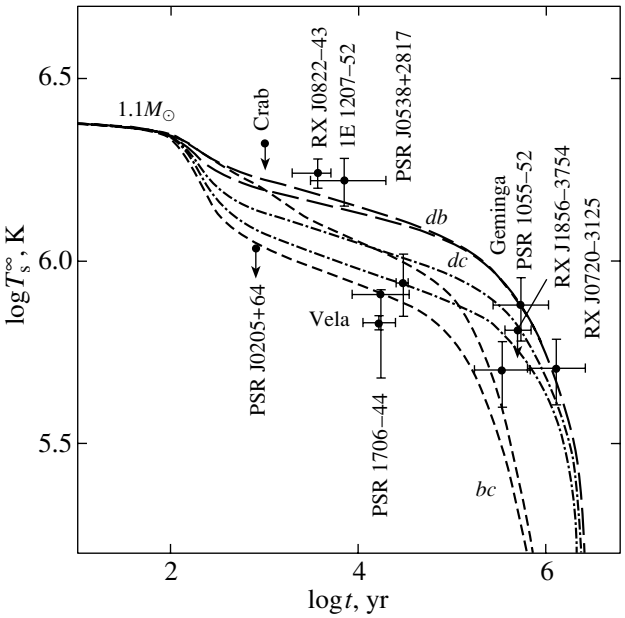

Fig. 7. Cooling curves of a low-mass ($M = 1.1\,M_\odot$) star for three nucleon superfluidity models (*db*, long dashes; *dc*, dashes and dots; *bc*, short dashes) in comparison with the observations. The lower and upper curves for each superfluidity model were computed with the renormalized ($\zeta_p = 1$) and nonrenormalized rate constant of neutrino energy release due to Cooper proton pairing, respectively.

The neutrino emission due to proton pairing plays a relatively minor role, and the exact value of ζ_p weakly affects the cooling.

In the *dc* and, particularly, the *bc* model, moderate proton pairing $\beta = c$ results in intense neutrino emission and appreciably speeds up the cooling. In these cases, the cooling curves are most sensitive to ζ_p. However, as we see from Fig. 7, the ζ_p variations considered cannot lead to agreement of the *dc* and *bc* cooling curves with the observations and, hence, do not affect our conclusions. We believe the renormalized value of $\zeta_p = 1$ to be more realistic than its nonrenormalized value. The existing uncertainty in ζ_p introduces uncertainty into the cooling theory. In particular, for the nonrenormalized value of ζ_p, the approximate symmetry of the cooling curves relative to the inversion of the models of nucleon superfluidity $\alpha\beta$ and $\beta\alpha$ noted above is much less pronounced than that for the renormalized value (see also Yakovlev *et al.* 1999a). The choice of ζ_p may subsequently prove to be important for reconciling the theory with the observations.

THE TWO TYPES OF NEUTRON TRIPLET SUPERFLUIDITY

Let us compare the influence of the two types of neutron triplet superfluidity (B and C) on the cooling

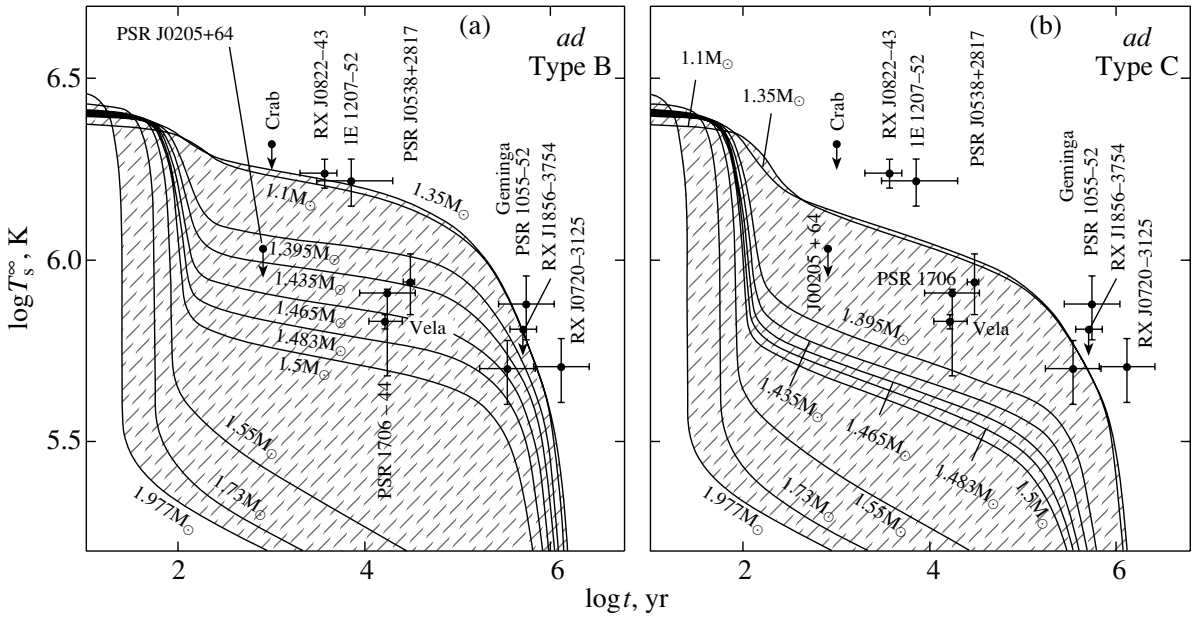

Fig. 8. Same as Fig. 2 for the model *a* of strong type-B (a) and type-C (b) superfluidity and the model *d* of weak proton superfluidity.

of neutron stars. Clearly, significant differences might be expected for strong neutron superfluidity. As follows from the results of the previous section, strong type-B neutron superfluidity (the model *a*) with weak proton superfluidity (the model *d*) can ensure agreement between the theory and the observations. Let us consider this case in more detail. Figure 8 shows the cooling curves for neutron stars of different masses with superfluidity *ad*: in panels (a) and (b), we took the type-B and type-C neutron pairing models, respectively.

It follows from an examination of Fig. 8a that, just as for the *da* model (Fig. 2), we can identify the same three types of cooling neutron stars: *low-mass*, slowly cooling stars; *high-mass*, rapidly cooling stars; and *medium-mass* stars with a moderate cooling rate.

The cooling of neutron stars with type-C neutron superfluidity was first calculated by Schaab *et al.* (1998). However, these authors used an oversimplified description of the influence of superfluidity on the neutrino reactions. More accurate calculations were performed by Gusakov and Gnedin (2002), who compared the results obtained for type-B and -C superfluidities. The authors used the approximation of constant critical temperatures $T_{\rm cp}$ and $T_{\rm cnt}$ over the stellar core. Calculations indicate that, in many cases, the shape of the cooling curves does not change if effective constant critical temperatures close to $T_{\rm cp}(\rho_{\rm c})$ and $T_{\rm cnt}(\rho_{\rm c})$ at the stellar center ($\rho = \rho_{\rm c}$) are used in place of the actual $T_{\rm cp}(\rho)$ and $T_{\rm cnt}(\rho)$ profiles. This approximation is valid when $T_{\rm c}(\rho)$ changes smoothly near the stellar center (e.g., in low-mass stars).

Gusakov and Gnedin (2002) showed that type-C neutron superfluidity speeds up the neutron-star cooling (compared to type-B superfluidity). This is attributable to the power-law suppression of the neutrino processes by type-C superfluidity (in contrast to the exponential suppression in case B; see, e.g., Yakovlev *et al.* 1999a; Gusakov 2002). Our calculations (Fig. 8) indicate that the above conclusion also remains valid in a more realistic approach that takes into account the variations of the critical temperatures $T_{\rm cnt}(\rho)$ and $T_{\rm cp}(\rho)$ over the stellar core.

The cooling curves for low- and medium-mass stars in Fig. 8b lie well below those for stars of the same masses in Fig. 8a. On the other hand, the cooling curves for high-mass ($M \gtrsim 1.55\ M_\odot$) stars in both panels of the figure almost coincide for the obvious reason: the critical temperatures are low in the central regions of these stars ($T_{\rm cnt} \lesssim 10^8$ K, see Fig. 1), so the superfluidity ceases to affect the cooling altogether.

Thus, according to Fig. 8, strong type-C neutron superfluidity disagrees with the observations of the hottest neutron stars for their ages. This superfluidity is still too weak to completely suppress the modified URCA process in a low-mass star, thereby making the star hotter. Of course, the theory can be reconciled with the observations by choosing the model of stronger type-C superfluidity. Our calculations indicate that this requires a $T_{\rm cnt}(\rho)$ profile with the maximum at $T_{\rm cnt}^{\rm max} \sim 10^{11}$ K. However, such strong triplet

superfluidity seems unrealistic. Khodel *et al.* (1998, 2001) gave theoretical arguments against the emergence of type-C superfluidity in neutron stars.

CONCLUSIONS

We have analyzed the cooling of neutron stars with neutron triplet superfluidity and proton singlet superfluidity in their cores. Our results are summarized below.

(1) The cooling curves for neutron stars are qualitatively symmetric relative to the inversion of the neutron and proton superfluidity models. For low-mass ($M < M_{\rm D}$) stars, this symmetry is largely determined by the dimensionless constant $\zeta_p \sim 1$ in the expression for the rate of neutrino energy release due to Cooper proton pairing. At $\zeta_p \ll 1$, obtained without the renormalization of ζ_p including multipartice effects, the symmetry is much less distinct than it is at $\zeta_p \sim 1$, which might be expected after renormalization.

(2) Two types of neutron and proton superfluidity models are consistent with the observations of thermal emission from isolated neutron stars. First, these include the models of strong (type A) proton superfluidity and weak (or completely absent) (type B or C) neutron superfluidity with maximum (over the stellar core) critical temperatures $T_{\rm cp}^{\rm max} \gtrsim 4 \times 10^9$ K and $T_{\rm cnt}^{\rm max} \lesssim 2 \times 10^8$ K. Second, these include the models of strong (type B) neutron superfluidity and weak (or completely absent) proton superfluidity with $T_{\rm cnt}^{\rm max} \gtrsim 5 \times 10^9$ K and $T_{\rm cp}^{\rm max} \lesssim 2 \times 10^8$ K. The models of the first type seem more realistic. Let us note, in particular, a recent paper by Schwenk and Friman (2004), who predicted a weakening of the neutron triplet pairing by effects of the medium.

(3) The models of moderate (type B or C) neutron superfluidity and/or moderate (type A) proton superfluidity with maximum critical temperatures $T_{\rm cnt}^{\rm max}$ and $T_{\rm cp}^{\rm max}$ in the range $\sim 2 \times 10^8$ to $\sim 4 \times 10^9$ K are inconsistent with the observations of primarily the hottest young neutron stars RX J0822−4300 and 1E 1207.4−5209. However, as was shown by Gusakov *et al.* (2004), there is a narrow region of model neutron and proton superfluidity parameters at which agreement between the cooling theory and the observations is also possible for moderate neutron superfluidity ($T_{\rm cnt}^{\rm max} \sim 6 \times 10^8$ K). This possibility was considered Gusakov *et al.* (2004).

(4) Strong type-C neutron triplet superfluidity can appreciably speed up the cooling of middle-aged ($10^3 \lesssim t \lesssim 10^5$ yr) neutron stars compared to type-B superfluidity for the same $T_{\rm cnt}(\rho)$ profiles. For strong type-C neutron superfluidity ($T_{\rm cnt}^{\rm max} \sim 5 \times 10^9$ K) and weak proton superfluidity ($T_{\rm cp}^{\rm max} \lesssim 2 \times 10^8$ K), the theory can no longer be reconciled with the observations of RX J0822−4300, 1E 1207.4−5209, PSR B1055−52, and RX J0720.4−3125, the hottest sources for their ages. For any models of strong or moderate neutron superfluidity, the transition from type-B to type-C superfluidity just enhances the difference between the theory and the observations.

Our analysis is simplified, because we considered only the cores of neutron stars composed of neutrons, protons, and electrons (disregarding the possible existence of hyperons, pion and kaon condensates, or quark matter). Moreover, we chose only one equation of state for matter in the cores of neutron stars and similar profiles of the critical neutron and proton temperatures $T_{\rm c}(\rho)$ in the stellar cores. Varying the equation of state (for the same composition of the matter) leads to a shift in the switch-on threshold of the direct URCA process (to a change in $\rho_{\rm D}$ and $M_{\rm D}$). Varying the $T_{\rm c}(\rho)$ profiles (with their general shape retained) at high $T_{\rm c}^{\rm max} \gtrsim 2 \times 10^9$ K leads to shifts in the characteristic values of ρ at which the superfluidity weakens and ceases to suppress the intense neutrino emission. Both lead to shifts in the boundary masses that separate the three types of cooling neutron stars (Kaminker *et al.* 2002), but do not alter our main conclusions. Significantly, the simplest model of neutron stars with strong proton superfluidity (even without neutron superfluidity) is capable of explaining the available observations.

It should be noted that the cooling of neutron stars also depends on the (singlet) neutron superfluidity in the inner stellar crust, on the magnetic field in the outermost stellar layers, and on the presence or absence of a surface layer of light elements (see, e.g., Potekhin *et al.* 2003). In general, however, these factors have a weaker effect on the cooling than the nucleon superfluidity in the cores of neutron stars considered here. We disregarded them by restricting our analysis to the superfluidity effects in the stellar cores. Our cooling code allows these factors to be easily taken into account, and this may be necessary for interpreting individual sources, primarily the hottest objects for their ages (see, e.g., Potekhin *et al.* 2003). The cooling of neutron stars may also depend on the stellar heating mechanisms related, for example, to the viscous dissipation of differential rotation energy (see, e.g., Page 1998a, 1998b). We emphasize that these heating mechanisms are model dependent. At the same time, the available observations can also be interpreted without invoking them.

Note that the surface temperatures of neutron stars $T_{\rm s}^{\infty}$ are difficult to determine from observational data (see, e.g., Pavlov *et al.* 2002). Reliable observational data and theoretical models of neutron star atmospheres are required to solve this problem.

The existing values of T_s^∞ can change appreciably, which can strongly affect the offered interpretation of the observations of primarily RX J0822–4300, 1E 1207.4–5209, PSR B1055–52, and RX J0720.4–3125. Future observations of the thermal emissions from isolated neutron stars will be crucial in understanding the superfluidity properties of dense matter in stellar cores.

ACKNOWLEDGMENTS

This work was supported by the Russian Foundation for Basic Research (project nos. 02-02-17668 and 03-07-90200), the Russian Leading Scientific Schools Program (project no. 1115.2003.2), and the INTAS YSF (grant no. 03-55-2397).

REFERENCES

1. L. Amundsen and E. Østgaard, Nucl. Phys. A **442**, 163 (1985).
2. R. G. Arendt, E. Dwek, and R. Petre, Astrophys. J. **368**, 474 (1991).
3. M. Baldo, J. Cugnon, A. Lejeune, and U. Lombardo, Nucl. Phys. A **536**, 349 (1992).
4. T. M. Braje and R. W. Romani, Astrophys. J. **580**, 1043 (2002).
5. W. F. Brisken, S. E. Thorsett, A. Golden, and W. M. Goss, Astrophys. J. Lett. **593**, L89 (2003).
6. V. Burwitz, F. Haberl, R. Neuhäuser, *et al.*, Astron. Astrophys. **399**, 1109 (2003).
7. G. W. Carter and M. Prakash, Phys. Lett. B **525**, 249 (2002).
8. E. G. Flowers, M. Ruderman, and P. G. Sutherland, Astrophys. J. **205**, 541 (1976).
9. O. Y. Gnedin, D. G. Yakovlev, and A. Yu. Potekhin, Mon. Not. R. Astron. Soc. **324**, 725 (2001).
10. M. E. Gusakov, Astron. Astrophys. **389**, 702 (2002).
11. M. E. Gusakov and O. Yu. Gnedin, Astron. Lett. **28**, 669 (2002).
12. M. E. Gusakov, A. D. Kaminker, D. G. Yakovlev, and O. Y. Gnedin, Astron. Astrophys. **606**, 444 (2004); astro-ph/0404002.
13. P. Haensel, *Final Stages of Stellar Evolution,* Ed. by J.-M. Hameury and C. Motch (EAS Publ. Ser. EDP Sci., 2003), p. 249.
14. A. D. Kaminker, P. Haensel, and D. G. Yakovlev, Astron. Astrophys. **345**, L14 (1999).
15. A. D. Kaminker, P. Haensel, and D. G. Yakovlev, Astron. Astrophys. **373**, L17 (2001).
16. A. D. Kaminker, D. G. Yakovlev, and O. Y. Gnedin, Astron. Astrophys. **383**, 1076 (2002).
17. D. L. Kaplan, S. R. Kulkarni, M. H. van Kerkwijk, and H. L. Marshall, Astrophys. J. Lett. **570**, L79 (2002).
18. V. A. Khodel, J. W. Clark, and M. V. Zverev, Phys. Rev. Lett. **87**, 031103 (2001).
19. V. A. Khodel, V. V. Khodel, and J. W. Clark, Phys. Rev. Lett. **81**, 3828 (1998).
20. M. Kramer, A. G. Lyne, G. Hobbs, *et al.*, Astrophys. J. Lett. **593**, L31 (2003).
21. J. M. Lattimer, C. J. Pethick, M. Prakash, and P. Haensel, Phys. Rev. Lett. **66**, 2701 (1991).
22. J. M. Lattimer and M. Prakash, Astrophys. J. **550**, 426 (2001).
23. K. P. Levenfish, Yu. A. Shibanov, and D. G. Yakovlev, Pis'ma Astron. Zh. **25**, 491 (1999) [Astron. Lett. **25**, 417 (1999)].
24. U. Lombardo and H.-J. Schulze, *Physics of Neutron Star Interiors,* Ed. by D. Blaschke *et al.* (Springer, Berlin, 2001), p. 30.
25. A. G. Lyne, R. S. Pritchard, F. Graham-Smith, and F. Camilo, Nature **381**, 497 (1996).
26. K. E. McGowan, S. Zane, M. Cropper, *et al.*, Astrophys. J. **600**, 343 (2004).
27. N. Motch, V. E. Zavlin, and F. Haberl, Astron. Astrophys. **408**, 323 (2003).
28. D. Page, NATO ASI Ser. C **515**, 539 (1998).
29. D. Page, *Neutron Stars and Pulsars*, Ed. by N. Shibazaki *et al.* (Univ. Acad. Press, Tokyo, 1998), p. 183.
30. G. G. Pavlov and V. E. Zavlin, in *Proceedings of the XXI Texas Symposium on Relativistic Astrophysics,* Ed. by R. Bandiera *et al.* (World Sci., Singapore, 2003), p. 319.
31. G. G. Pavlov, V. E. Zavlin, D. Sanwal, *et al.*, Astrophys. J. Lett. **552**, L129 (2001).
32. G. G. Pavlov, V. E. Zavlin, and D. Sanwal, *WE-Heraeus Seminar on Neutron Stars, Pulsars and Supernova Remnants No. 270*, Ed. by W. Becker *et al.* (MPE-Report No. 278, Garching, 2002), p. 273.
33. J. A. Pons, F. Walter, J. Lattimer, *et al.*, Astrophys. J. **564**, 981 (2002).
34. A. Y. Potekhin, D. G. Yakovlev, G. Chabrier, and O. Y. Gnedin, Astrophys. J. **594**, 404 (2003).
35. M. Prakash, T. L. Ainsworth, and J. M. Lattimer, Phys. Rev. Lett. **61**, 2518 (1988).
36. R. S. Roger, D. K. Milne, M. J. Kesteven, *et al.*, Astrophys. J. **332**, 940 (1988).
37. Ch. Schaab, F. Weber, and M. K. Weigel, Astron. Astrophys. **335**, 596 (1998).
38. A. Schwenk and B. Friman, Phys. Rev. Lett. **92**, 082501 (2004).
39. P. O. Slane, D. J. Helfand, and S. S. Murray, Astrophys. J. Lett. **571**, L45 (2002).
40. J. E. Trümper, V. Burwitz, F. Haberl, and V. E. Zavlin, astro-ph/0312600 (2003).
41. F. M. Walter, Astrophys. J. **549**, 433 (2001).
42. F. M. Walter and J. M. Lattimer, Astrophys. J. Lett. **576**, L145 (2002).
43. M. C. Weisskopf, S. L. O'Dell, F. Paerels, *et al.*, Astrophys. J. **601**, 1050 (2004).
44. P. F. Winkler, J. H. Tuttle, R. P. Kirshner, and M. J. Irwin, *Supernova Remnants and the Interstellar Medium,* Ed. by R. S. Roger and T. L. Landecker (Cambridge Univ. Press, Cambridge, 1988), p. 65.
45. D. G. Yakovlev, O. Y. Gnedin, A. D. Kaminker, and A. Y. Potekhin, *WE-Heraeus Seminar on Neutron Stars, Pulsars and Supernova Remnants No. 270*, Ed. by W. Becker *et al.* (MPE-Report No. 278, Garching, 2002), p. 287.

46. D. G. Yakovlev, A. D. Kaminker, and O. Y. Gnedin, Astron. Astrophys. **379**, L5 (2001).
47. D. G. Yakovlev, A. D. Kaminker, O. Y. Gnedin, and P. Haensel, Phys. Rep. **354**, 1 (2001).
48. D. G. Yakovlev, A. D. Kaminker, and K. P. Levenfish, Astron. Astrophys. **343**, 650 (1999).
49. D. G. Yakovlev, K. P. Levenfish, and Yu. A. Shibanov, Usp. Fiz. Nauk **169**, 825 (1999).
50. S. Zane, F. Haberl, M. Cropper, *et al.*, Mon. Not. R. Astron. Soc. **334**, 345 (2002).
51. V. E. Zavlin and G. G. Pavlov, in *Proceedings of the EPIC Consortium, Palermo, Oct. 14–16, 2003*; astro-ph/0312326 (2003).
52. V. E. Zavlin, G. G. Pavlov, and D. Sanwal, Astrophys. J. **606**, 444 (2004); astro-ph/0312096.
53. V. E. Zavlin, J. Trümper, and G. G. Pavlov, Astrophys. J. **525**, 959 (1999).

Translated by V. Astakhov